
Masked Image Modeling with Denoising Contrast

Kun Yi^{1*} Yixiao Ge^{1*} Xiaotong Li^{1,2†} Shusheng Yang^{1,3†}
 Dian Li⁴ Jianping Wu⁶ Ying Shan¹ Xiaohu Qie⁵

¹ARC Lab, ⁵Tencent PCG

²Peking University ³Huazhong University of Science and Technology

⁴Content Understanding Center, ⁵Tencent PCG ⁶Tsinghua University

Abstract

Since the development of self-supervised visual representation learning from contrastive learning [17, 4] to masked image modeling [1, 9], there is no significant difference in essence, that is, how to design proper pretext tasks for vision dictionary look-up. Masked image modeling recently dominates this line of research with state-of-the-art performance on vision Transformers [10], where the core is to enhance the patch-level visual context capturing of the network via denoising auto-encoding mechanism. Rather than tailoring image tokenizers with extra training stages as in previous works [1, 9, 21], we unleash the great potential of contrastive learning on denoising auto-encoding and introduce a new pre-training method, ConMIM, to produce simple intra-image inter-patch contrastive constraints as the learning objectives for masked patch prediction. We further strengthen the denoising mechanism with asymmetric designs, including image perturbations and model progress rates, to improve the network pre-training. ConMIM-pretrained vision Transformers with various scales achieve promising results on downstream image classification, semantic segmentation, object detection, and instance segmentation tasks, *e.g.*, we achieve 83.7% top-1 accuracy with ViT-Base and 82.0% with ViT-Small on ImageNet-1K [7] classification.

1 Introduction

The great success of self-supervised learning in natural language processing (NLP) tasks, *e.g.*, BERT [8] and GPT [27, 28], has sparked several revolutions in visual representation learning, during which the development of *vision dictionary look-up* is the most critical. In the age of convolutional neural networks (CNNs) [19, 20, 32], prominent works [17, 4] perform self-supervised learning with a pretext task of *instance-level dictionary look-up via contrastive learning* as demonstrated in Figure 1(a). With the advent of vision Transformers (ViTs) [10, 31, 25], the gap between vision and NLP tasks has been further narrowed since the introduction of *patch-level dictionary look-up via masked image modeling* in a pioneer work BEiT [1] (see Figure 1(b)).

The introduction of masked image modeling [1], inspired by masked language modeling [8] in NLP tasks, ushers in a new fad for self-supervised learning using vision Transformers [10], *i.e.*, a portion of vision tokens are randomly masked and then recovered by the Transformer network being trained. Concurrent works [9, 21] make efforts to design patch-level dictionaries, image tokenizers in other words, to build proper learning objectives (*i.e.*, vision token ids) for masked image modeling. Though advanced results can be achieved, the off-the-shelf image tokenizers, *e.g.*, discrete VAE [29] used in BEiT [1], depend on extra training stages and data knowledge, rendering an inflexible two-stage pre-training paradigm.

*Equal contribution. Contact: {kunyi, yixiaoge}@tencent.com

†Work done during Xiaotong and Shusheng’s internships in ARC Lab, Tencent PCG.

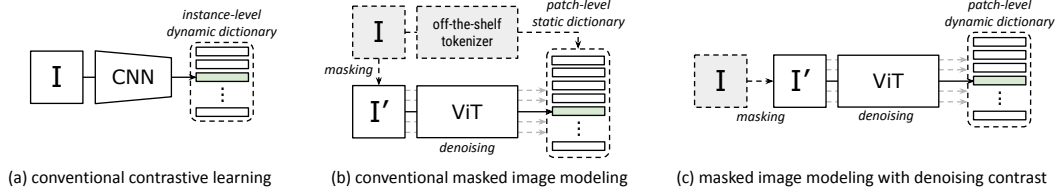


Figure 1: Conventional contrastive learning methods (e.g., MoCo [17], SimCLR [4]) and masked image modeling methods (e.g., BEiT [1], PeCo [9]) both perform the pretext task of vision dictionary look-up, where the superiority of the latter ones lie in the patch-level denoising auto-encoding mechanism to enable fine-grained visual context understanding of vision Transformers [10]. We introduce to cast masked image modeling as denoising contrastive learning to avoid the extra training stages of image tokenizer, rendering a flexible, simple and effective pre-training paradigm.

We would like to call for a revisit of the superiority of masked image modeling over contrastive learning on self-supervised learning with vision Transformers. Since they are essentially both designed towards vision dictionary look-up, the key difference lies in the patch-level denoising auto-encoding mechanism in masked image modeling, which encourages the network’s capability to capture fine-grained visual context and semantics. As for the auto-encoding objective, we do not have to intentionally discretize the continuous visual signals as words in NLP tasks to cast the masked prediction as a classification task. Instead, we can give full play to the wisdom of contrastive learning, which has good capability to structure the visual space with semantically meaningful representations. To this end, we introduce a new pre-training method for masked image modeling, namely, ConMIM, to get rid of extra tokenizing networks by revitalizing contrastive learning, as shown in Figure 1(c).

Our ConMIM casts masked patch prediction in self-supervised image pre-training as denoising contrastive learning. The corrupted input with a large proportion of patches masked is fed into the encoder, a plain vision Transformer in general. The encoder learns to recover the representations of the masked patches, which are predicted by feeding the full input into the encoder. The training objective is formed by an intra-image inter-patch contrastive loss. To be specific, patch representations of a full input image build a dynamic dictionary, and patches from the same positions as the masked ones of the corrupted input serve as their positive keys, respectively. The remaining ones from different positions but in a same image are the negative keys. To further improve the network via a stronger denoising auto-encoding mechanism, we introduce asymmetric designs in ConMIM training, including asymmetric image perturbations and asymmetric model progress rates. We adopt a strong augmentation for the full input while a weak augmentation for the corrupted input. For the image encoder, the slowly progressing momentum encoder [17] is employed for the full input to embed more challenging but semantically consistent learning targets.

Empirically, we perform self-supervised learning with our ConMIM on the widely-acknowledged ImageNet-1K [7], and then fine-tune the pre-trained vision Transformers with various scales on four downstream tasks, *i.e.*, image classification, semantic segmentation, object detection and instance segmentation. With a vanilla ViT-Base model, we achieve 83.7% top-1 accuracy on ImageNet-1K classification. This outperforms the contrastive learning baseline MoCo v3 [6] and the masked image modeling baseline BEiT [1] without any auxiliary image tokenizer. When transferring ConMIM-pretrained models to downstream tasks, state-of-the-art performances can be consistently achieved. Other than the promising results, we would like to draw public attention to unleash the great potential of “outdated” contrastive learning in visual representation learning.

2 Related Work

Self-supervised learning via contrastive learning. The pretext task of contrastive learning [4, 17, 2] dominates self-supervised visual pre-training in the era of CNNs. Contrastive learning methods generally perform instance-level dictionary look-up. The anchors are pulled closer to their positive keys at the same time pushing away from the negative keys. The establishment of vision dictionaries is critical for the contrast regularization. For example, the seminal work MoCo [17] builds the vision dictionary with a first-in-first-out queue, driven by a momentum encoder. The concurrent work SimCLR [4] uses a large batch size to enlarge the dictionary with more negative keys. SwAV

[2] further introduces an online clustering algorithm in an unsupervised manner, and the cluster assignments serve for the dictionary keys. Despite the great achievements with CNNs, these methods are gradually abandoned with the introduction of ViTs [10]. This is mainly due to the lack of inductive bias in ViTs, which requires stronger supervision for better pre-training performance.

Another line of research on contrastive learning [38, 42, 41, 30] focuses on how to learn better pre-trained weights specifically for dense downstream tasks, *e.g.*, object detection and segmentation. They are mainly devoted to taking local feature representations into consideration. For instance, DenseCL [38] constructs a dense contrastive loss in pixel level to better preserve the spatial information. PixPro [42] introduces pixel-to-propagation consistency to employ contrastive loss at region level. These methods are related to our ConMIM in the perspective of refining the instance-level supervision into a more fine-grained patch level. However, they do not consider the denoising mechanism, which is the core of effective pre-training in ViTs.

Self-supervised learning via masked image modeling. With the introduction of Transformer architecture [10] in computer vision, researchers attempt to reproduce the success of masked language modeling [8] in self-supervised learning of vision Transformers. Specifically, BEiT [1] introduces a new pretext task, namely, masked image modeling, for visual pre-training. They tokenize high-dimensional images into discrete vision tokens by a discrete VAE [29] to establish a static patch-level dictionary as in NLP tasks. A proportion of image patches are randomly masked, the backbone network is then trained to recover the vision token ids of the masked patches, rendering a denoising mechanism. Follow-up works make efforts to further improve the static dictionaries, *e.g.*, mc-BEiT [21] introduces eased and refined dictionaries with multiple choices. PeCo [9] proposes to produce perceptual-aware keys in the patch-level dictionary. Though their results are promising, these methods all require extra training stages and even extra data for obtaining a proper image tokenizer.

There are other recent works that cast masked image modeling as a denoising pixel-level reconstruction task (*e.g.*, MAE [16]) or a self-distillation task (*e.g.*, iBOT [45]) rather than denoising dictionary look-up. They achieve state-of-the-art results without auxiliary tokenizers but require more training epochs, *i.e.*, 1600 epochs for MAE vs. 800 epochs for BEiT when training with ViT-Base. The reason might be that the reconstruction loss or the regression loss in these methods is more eased than the classification loss or the contrastive loss in dictionary look-up, leading to the requirement of more iterations for the optimal performance. A similar situation has appeared in the era of CNNs. BYOL [15] uses only regression loss for image pre-training while neglecting the negative pairs because gathering negative samples in contrastive loss requires extra multi-machine communication costs. However, things become different in masked image modeling. Our ConMIM shows that intra-image negative keys are sufficient enough to fully regularize the network without increasing computational overhead or training epochs compared to the vanilla BEiT.

3 Preliminaries

The pretraining-and-then-finetuning paradigm has been proven to be effective for visual representation learning and various downstream tasks, where self-supervised pre-training [17, 4, 3, 2, 5, 15, 1, 9, 16, 39, 43, 45, 13, 36] is the most popular. Since there are no ground-truth annotations available, the design of pretext tasks is critical to the pre-training performance. Though driven by various motivations and progressing architectures [20, 19, 10], the pretext task of visual self-supervised learning is essentially to perform vision dictionary look-up, inspired by the success of NLP tasks [8, 27, 28].

3.1 Contrastive Learning: Instance-level Vision Dictionary Look-up

From the perspective of vision dictionary look-up, prominent contrastive learning methods establish instance-level vision dictionaries via a fixed-length queue [17] or batch-wise samples [4]. The keys in the dictionary are dynamically updated as pre-training proceeds. Given an image x , its feature representation is encoded by feeding it into the backbone network, *i.e.*, $f(x)$. An InfoNCE loss [35] is employed to regularize this representation, bringing it closer to its positive key k_+ while staying away from negative keys, denoted as

$$\mathcal{L}_{\text{con}}(x) = -\log \frac{\exp(\langle f(x), k_+ \rangle / \tau)}{\sum_{i=1}^K \exp(\langle f(x), k_i \rangle / \tau)}, \quad (1)$$

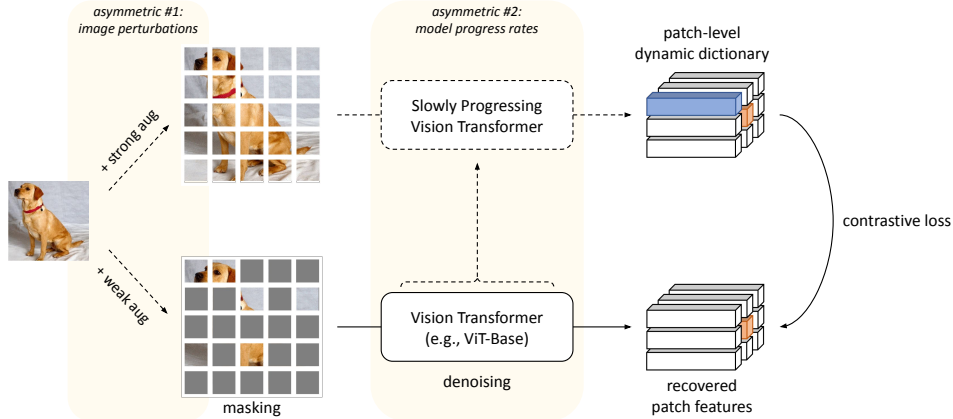


Figure 2: Our ConMIM performs the masked patch prediction with denoising contrast, coupling with two asymmetric designs to achieve state-of-the-art performance on self-supervised image pre-training. The slowly progressing vision Transformer is a snapshot of the backbone network under training, and we do not require any off-the-shelf image tokenizers [29, 11]. The training objective of denoising contrastive loss performs a patch-level look-up from dynamic vision dictionaries and enhances the network’s capability to capture more fine-grained visual context.

where $\langle \cdot, \cdot \rangle$ indicates the cosine similarity measured by the dot product between two L_2 -normalized features, τ is the temperature hyper-parameter and K is the dictionary size. Generally, the positive key is built by another view of the same instance [33], *e.g.*, different image augmentations.

3.2 Masked Image Modeling: Patch-level Vision Dictionary Look-up

With the popularity of Transformer architectures [10] in computer vision tasks, the pretext task of masked image modeling gradually dominates visual representation learning. It randomly masks a large percentage of image patches and trains the backbone network to recover the token ids of corrupted image via more fine-grained patch-level vision dictionary look-up. The dictionary is generally static and pre-defined by an off-the-shelf image tokenizer [29, 11], which converts continuous visual signals into discrete keys. For example, in the seminal work BEiT [1], a pre-learned discrete VAE [29] is adopted as the tokenizer. The masked patch prediction is then cast as a classification task with cross-entropy loss,

$$\mathcal{L}_{\text{mim}}(x) = \mathbb{E}_{j \in \mathcal{M}} [-\log p(y_j | f(\hat{x})_j)], \quad (2)$$

where \mathcal{M} denotes the set of masked patch indices, \hat{x} is the corrupted image after randomly masking, y_j is the positive key index in the patch-level dictionary, and $p(\cdot | \cdot)$ indicates the probability that correctly identifies the recovered patch $f(\hat{x})_j$ with a patch index of j .

4 Masked Image Modeling with Denoising Contrast

Despite that existing contrastive learning and masked image modeling methods optimize the backbone network towards different training objectives (*i.e.*, InfoNCE loss and cross-entropy loss), they both attempt to learn discriminative visual representations via dictionary look-up. Two key factors lead to the state-of-the-art performance of masked image modeling. (1) More fine-grained supervision from instance-level to patch-level benefits the vision Transformer architecture known for its data-hungry properties. (2) The denoising auto-encoding mechanism, formed by the masking-and-then-predicting paradigm, encourages the capability of the backbone network to capture visual context and perceptions. Though promising results are achieved by existing masked image modeling methods [1, 9, 21], they require extra training stages to establish static vision dictionaries with offline image tokenizers.

Towards this end, we call for a revitalization of contrastive learning, which has good capability to structure the latent space for self-supervised representation learning. A new self-supervised pre-training method, ConMIM, is introduced to perform masked image modeling with denoising

contrastive objectives while eliminating the dependence on pre-learned image tokenizers, as illustrated in Figure 2.

Patch-level dynamic dictionary. We build dynamic patch-level dictionaries to form the learning targets for masked patch prediction on-the-fly. Specifically, during each training iteration, the full input image x is fed into the backbone network to embed the patch feature representations, serving as keys in the dynamic dictionary, *i.e.*, $\{f(x)_i\}_{i=1}^K$ where i is the patch index, K is the dictionary size as well as the total number of patches within an image (*e.g.*, $K = 196$ keys for a 224×224 image with a patch size of 16×16). Without the loss of representation discriminativeness, we build separate dictionaries for each image, that is, only operate patch-level dictionary look-up within each image. We discuss this design in Sec. 5.4.2 with ablation studies using a larger or smaller dictionary size, where inferior results are achieved and require extra computational overhead.

Denosing contrastive objective. The corrupted image, \hat{x} , is then fed into the backbone network, and we denote the encoded patch feature representation of a certain masked patch as $f(\hat{x})_j, j \in \mathcal{M}$. The backbone network is trained to denoise the corrupted image and recover the masked patches through visual context reasoning. The masked patch recovery is regularized by a patch-level dictionary look-up in the form of an InfoNCE loss [35],

$$\mathcal{L}_{\text{conmim}}(x) = \mathbb{E}_{j \in \mathcal{M}} \left[-\log \frac{\exp(\langle f(\hat{x})_j, \text{sg}[f(x)_j] \rangle / \tau)}{\sum_{i=1}^K \exp(\langle f(\hat{x})_j, \text{sg}[f(x)_i] \rangle / \tau)} \right], \quad (3)$$

where $\text{sg}[\cdot]$ indicates stop-gradient operation. We only backpropagate the gradients of the corrupted inputs $f(\hat{x})$ because backpropagating the gradients of the full input $f(x)$ may lead to information leakage and useless denoising. With the above training objectives, the backbone network is encouraged to better capture the visual context and learns to encode local discriminative representations.

Asymmetric design. As patches (*e.g.*, 16×16) are small-scale inputs with less useful information and highly redundant semantics, we need to make the pre-training task more challenging to improve the backbone network. Towards this goal, the recent work MAE [16] proposes to mask a large proportion of patches. In our work, besides the large proportion of patch dropout, we further introduce two asymmetric designs to enable a stronger denoising regularization during pre-training.

(1) *Asymmetric image perturbations.* We adopt different data augmentations for the full input image x and the corrupted image \hat{x} before feeding into the backbone network. To be specific, we utilize stronger augmentations for the full input image referring to contrastive learning methods [4], including random flip, resize, crop, color distort, Gaussian blur, and solarization. And we only use basic augmentations for the corrupted image referring to masked image modeling methods [1], including random flip, resize, and crop. Note that we use the same flip, resize and crop operations for paired inputs in order to keep the patch positions consistent. We discuss the alternative options in Sec. 5.4.3. We observe that it is sub-optimal to use strong augmentations for corrupted images, and the reason might be that the strong perturbations would bias the network’s capability of capturing local context. A concurrent work [37] discusses the importance of asymmetric augmentations in MoCo v3 [6]. The empirical conclusion is opposite with our ConMIM, indicating the different characteristics of conventional contrastive learning and denoising contrastive learning.

(2) *Asymmetric model progress rates.* We employ different model progress rates of the backbone network for embedding the corrupted input and full input. We use the plain backbone network for the corrupted input while using its momentum updated version for the full input. The momentum encoder [17] is known as a slowly progressing model that can encode more challenging but semantically consistent key feature representations for building dictionaries. Specifically, we denote the model parameters of the backbone $f(\cdot)$ as θ and the model parameters of the momentum updated one as $\tilde{\theta}$. The momentum encoder is updated via $\tilde{\theta} = (1 - \alpha)\theta + \alpha\tilde{\theta}$ in each iteration, where $\alpha \in [0, 1]$ is the momentum coefficient. Larger momentum coefficients indicate slower model progress.

Pre-training setup. ConMIM pre-training is conducted on the training set of ImageNet-1K [7] dataset in a self-supervised manner. We utilize ViT-S/16 and ViT-B/16 [10] as the backbone networks. Following MoCo v3 [6], we use a 3-layer projection head on top of the backbone network for pre-training and discard it when transferring to downstream tasks. The input images are all resized to 224×224 and the patch size is set to 16×16 . We follow the masking strategy of MAE [16], *i.e.*,

Methods	Image Size	Pre-training Epoch	ImageNet [7] Top-1
<i>Training from scratch</i>			
DeiT-S [34]	224 ²	-	79.8
DeiT-B [34]	224 ²	-	81.8
DeiT-B [34]	384 ²	-	83.1
<i>Self-supervised pre-training using ViT-S/16 [10]</i>			
MoCo v3 [6]	224 ²	300	81.4
DINO [3]	224 ²	800	81.5
MAE [16]†	224 ²	800	80.9
CIM [12]	224 ²	300	81.6
BEiT [1]	224 ²	300	81.3
ConMIM (Ours)	224 ²	300	82.0
ConMIM (Ours)*	384 ²	300	83.9
<i>Self-supervised pre-training using ViT-B/16 [10]</i>			
MoCo v3 [6]	224 ²	300	83.2
DINO [3]	224 ²	800	82.8
MAE [16]	224 ²	1600	83.6
CIM [12]	224 ²	300	83.3
BEiT [1]	224 ²	300	82.9
BEiT [1]	224 ²	800	83.2
BEiT [1]*	384 ²	800	84.6
ConMIM (Ours)	224 ²	300	83.5
ConMIM (Ours)	224 ²	800	83.7
ConMIM (Ours)*	384 ²	800	85.3

Table 1: Top-1 accuracy (%) on ImageNet-1K [7] classification using ViT-Small and ViT-Base models. (*) The resolution of 384² is only used for fine-tuning. We follow the same 384² fine-tuning setup of BEiT [1], *i.e.*, after fine-tuning with 224², another 10% epochs are further used for fine-tuning on 384². All the models use 224² images for pre-training. (†) Reproduced result with official code.

75% patches are randomly masked. The learning rate is set to 5e-4, with a warmup of 10 epochs, and cosine learning rate decay. The temperature τ is set to 0.1 and the momentum coefficient α is initially set to 0.996 with a cosine scheduler. ViT-B/16 is pre-trained for 800 epochs in total and ViT-S/16 is pre-trained for 300 epochs if not specified. The other hyper-parameters are mostly the same as BEiT [1]. More implementation details can be found in Appendix B.1.

5 Experiments

We further evaluate the models pre-trained by our ConMIM on different downstream tasks, including image classification on ImageNet-1K [7] (Sec. 5.1), semantic segmentation on ADE20K [44] (Sec. 5.2), object detection and instance segmentation on COCO [24] (Sec. 5.3). We further discuss the key components and hyper-parameters in ConMIM pre-training via ablation studies in Sec. 5.4.

5.1 Image Classification

We test our ConMIM by fine-tuning the pre-trained models on ImageNet-1K [7] classification, which contains 1.3M images out of 1K classes in total. We follow the fine-tuning setup of state-of-the-art methods, *i.e.*, BEiT [1] for ViT-Base and CIM [12] for ViT-Small. They are almost identical except for training epoch and layer decay. To be specific, we use 100 epochs with a warm-up of 20 epochs, and a layer decay of 0.65 for ViT-Base fine-tuning. 200 epochs with a warm-up of 5 epochs and a layer decay of 0.8 for ViT-Small fine-tuning. More hyper-parameters can be found in Appendix B.2.

We illustrate the evaluation results in Table 1. We observe that models with pre-trained weights overwhelmingly outperform the ones trained from scratch by DeiT [34], demonstrating the significance of self-supervised visual representation learning. Compared to the pioneering work of masked image modeling, BEiT [1], we consistently outperform it when fine-tuning on ViT-Base and ViT-Small models with both image resolutions of 224 × 224 and 384 × 384. Moreover, we do not require any extra tokenizing networks as in BEiT, realizing more efficient and flexible one-stage pre-training.

Methods	ADE20K [44] mIOU
<i>Backbone using ViT-S/16 [10]</i>	
BEiT [1]*	46.3
ConMIM (Ours)*	47.7
<i>Backbone using ViT-B/16 [10]</i>	
Supervised [34]	45.3
MoCo v3 [17]	47.2
DINO [3]	46.8
BEiT [1]*	47.7
ConMIM (Ours)*	49.8

Table 2: Semantic segmentation on ADE20K [44] in terms of mIOU (%). (*) Transferring after intermediate fine-tuning on ImageNet-1K [7], which is a common practice of BERT [8] in NLP.

Methods	opt. lr	COCO [24]	
		AP ^{box}	AP ^{mask}
<i>Backbone using ViT-S/16 [10]</i>			
DeiT [34]	8.0e-5	43.1	38.8
MAE [16]*	8.0e-5	41.5	37.8
ConMIM (Ours)*	1.0e-4	45.8	41.0
<i>Backbone using ViT-B/16 [10]</i>			
DeiT [34]	8.0e-5	46.5	41.7
DINO [3]	8.0e-5	47.6	42.3
MoCo v3 [6]	1.6e-4	47.3	42.2
MAE [16]*	8.0e-5	47.8	42.9
ConMIM (Ours)*	1.0e-4	48.7	43.6

Table 3: Object detection and instance segmentation on COCO [24] in terms of AP^{box} (%) and AP^{mask} (%). “opt. lr” indicates the optimal learning rate for each method. (*) With intermediate fine-tuning on ImageNet.

We also surpass the state-of-the-art contrastive learning methods, *e.g.*, MoCo v3 [6], indicating the superiority of denoising auto-encoding mechanism. The recent work MAE [16] casts masked image modeling as a pixel-level reconstruction work rather than vision dictionary look-up. As we discussed before, they require more training epochs for optimal performance as the regularization of pixel-level reconstruction loss is much more eased than the classification loss or the contrastive loss. Such flaws are especially evident in the performance of small-scale models, *i.e.*, ViT-Small. Another related work, iBOT [45], is conducted with multi-crop augmentation and thus not fair to be compared.

5.2 Semantic Segmentation

We evaluate ConMIM on the downstream semantic segmentation using ADE20K [44] benchmark, which consists of 25K images of 150 semantic categories. We use the evaluation metric, mean intersection over union (mIOU), for reference. We use UperNet [40] and adopt the same setup for ViT-Base and ViT-Small, which are mostly following BEiT [1] (find details in Appendix B.3). Images are resized to 512×512 as input, and the model is fine-tuned for 160K iterations in total. We also use intermediate fine-tuning to achieve the optimal results following BEiT [1], *i.e.*, first fine-tuning the pre-trained models on ImageNet-1K classification and then transferring to ADE20K. The results are shown in Table 2. We consistently surpass the baseline BEiT with significant improvements, *e.g.*, our 49.8% vs. BEiT’s 47.7% on ViT-Base. Moreover, our ConMIM using ViT-Small even achieves comparable performance with BEiT using ViT-Base, *i.e.*, 47.7%. Models pre-trained by masked image modeling generally achieve better performance on segmentation than the ones pre-trained by conventional contrastive learning, *e.g.*, MoCo v3 [6].

5.3 Object Detection and Instance Segmentation

For object detection and instance segmentation, we fine-tune Mask R-CNN [18] end-to-end on COCO [24]. We follow the implementation of [22] and reproduce all the results in Table 3 since [22] is still close-source. To tame quadratic complexity with self-attention, most attention blocks in the ViT backbone are replaced with windowed blocks except for four global blocks to perform cross-window interaction. Four up/down-sample modules are evenly placed with ViT to produce pyramid features required by FPN [23]. The training recipes keep the same with [22]. An input image is resized to 1024×1024 and augmented by large scale jitter [14], with a resize scale of [0.1, 2.0]. We fine-tune the pre-trained models for 25 epochs using an AdamW [26] optimizer with a weight decay of 0.1 and cosine learning rate scheduler. All experiments are performed under the same settings, except for the learning rate is specifically tuned for each model. Check hyper-parameters in Appendix B.4. We achieve much better performance than MAE [16], especially on the ViT-Small backbone.

5.4 Ablation Studies

In this section, we discuss component design in ConMIM through ablation studies. All the experiments in this section are conducted using ViT-B/16 [10] pre-trained for 300 epochs, and we report the top-1 classification accuracy after fine-tuning on ImageNet-1K [7].

5.4.1 Analysis of Denoising Auto-encoding Mechanism

Models	ImageNet [7] Top-1
DeiT-B [34] (<i>training from scratch</i>)	81.8
MoCo v3 [6] (<i>conventional contrastive learning</i>)	83.2
ConMIM (Ours)	83.51
denoising patch-level contrast \rightarrow vanilla instance-level contrast	82.26 (-1.25%)
denoising patch-level contrast \rightarrow vanilla patch-level contrast	<i>fail</i>

Table 4: Ablation studies on the effect of denoising auto-encoding mechanism.

The denoising auto-encoding mechanism is critical to the success of masked image modeling, where the fine-grained patch-level supervision and the masking-and-the-predicting paradigm are the two key factors. We conduct ablation studies in Table 4 to analyze their effect. (1) We remove the entire denoising auto-encoding mechanism from ConMIM, *i.e.*, using average local tokens to perform vanilla instance-level contrastive loss, significant performance drops (-1.25%) are observed. Such a result is even worse than MoCo v3 [6], the state-of-the-art method for conventional contrastive learning. (2) When only discarding the masking strategy while keeping patch-level contrast, the experiment totally fails due to the trivial information leakage with semantically repetitive patches.

5.4.2 Analysis of Patch-level Dynamic Dictionary

Models	ImageNet [7] Top-1
DeiT-B [34] (<i>training from scratch</i>)	81.8
ConMIM (Ours)	83.51
<i>more</i> : intra-image negative keys \rightarrow intra-gpu negative keys	82.60 (-0.91%)
<i>fewer</i> : intra-image negative keys \rightarrow filtered intra-image negative keys	83.12 (-0.39%)

Table 5: Ablation studies on the dictionary size of ConMIM.

ConMIM performs masked image modeling towards the objective of an intra-image inter-patch contrastive loss, *i.e.*, the dictionary is built individually for each image. The size of the dictionary has effects on the regularization of negative keys. We discuss such a design by either expanding the dictionary or reducing it, as shown in Table 5. (1) We expand the dictionary by gathering other images’ keys on the same GPU. Performance drops are observed. The reason might be that the keys from the same image share similar domains and serve as hard negatives for each other. Gathering more negatives from other domains actually ease the regularization. (2) Although patches within the same images can act as hard negatives, they might also be noisy negatives as patches are highly semantically redundant, *e.g.*, patches from different positions may carry similar patterns. So we try to filter them by excluding negative keys that are highly similar to the anchor patch in the latent space. Slight accuracy decreases are shown, indicating that we may exclude some valuable hard negatives. We acknowledge that, although ConMIM can achieve the state-of-the-art results to date, there should be room for further refinement in dictionary design. Further studies are called for.

5.4.3 Analysis of Asymmetric Designs

We introduce two asymmetric designs in ConMIM to enable a stronger denoising auto-encoding mechanism during pre-training. We discuss their effects in Table 6. (1) Asymmetric image perturbations. We use a stronger augmentation for the full input while the basic one for the corrupted image in ConMIM. We try to remove such asymmetric augmentation design and find slight performance drops when using either the stronger one or the basic one for both inputs. More significant performance drops can be observed when directly switching their augmentations. The reason might be the too difficult pretext task, *i.e.*, the backbone network needs to recover the strong-augmented corrupted input towards the full input targets with asymmetric perturbations. (2) Asymmetric model progress rates.

Models	ImageNet [7] Top-1
DeiT-B [34] (<i>training from scratch</i>)	81.8
ConMIM (Ours)	83.51
w/o asymmetric image perturbations, use stronger one	83.41 (-0.10%)
w/o asymmetric image perturbations, use basic one	83.35 (-0.16%)
w/ asymmetric image perturbations but switch	82.62 (-0.89%)
w/o asymmetric model progress rates	81.53 (-1.98%)

Table 6: Ablation studies on the effect of asymmetric designs.

We use a slowly progressing momentum model of the backbone network to embed more challenging but semantically consistent key representations. When removing such a design, noticeable accuracy decreases are shown, *i.e.*, -1.98%, which is even worse than DeiT [34] baseline.

5.4.4 Hyper-parameter Analysis

Masking Strategy	Masking Ratio	ImageNet [7] Top-1
Block	40%	82.12
	60%	83.20
	75%	83.11
	90%	82.63
Random	60%	82.52
	75%	83.51
	90%	83.04

Table 7: Ablation studies on different masking strategies and masking ratios.

temperature τ	ImageNet [7] Top-1
0.05	82.55
0.07	83.03
0.1	83.51
0.15	83.32
0.2	83.35

Table 8: Discuss temperature hyper-parameter in denoising contrastive loss.

momentum α	ImageNet [7] Top-1
0.99	83.11
0.996	83.51
0.999	83.31

Table 9: Discuss momentum coefficient in the slowly progressing model.

Masking ratio. The fine-tuning results on ImageNet using different masking strategies and ratios are shown in Table 7. Randomly masking at a ratio of 75% achieves the optimal performance.

Temperature. We discuss the effect of temperature hyper-parameter in our denoising contrastive loss (Eq. (3)), as illustrated in Table 8. $\tau = 0.1$ achieves the optimal performance empirically. We use this setup for both ViT-Small and ViT-Base.

Momentum. The fine-tuning accuracy on ImageNet using our ConMIM with different values of initial momentum coefficient is shown in Table 9. ConMIM is actually not sensitive to this hyper-parameter and we adopt 0.996 in all experiments for optimal performance.

6 Discussion and Conclusion

We present an intriguing perspective that masked image modeling [1, 9, 21] and contrastive learning [6, 17, 4] are essentially both pretext tasks for vision dictionary look-up. And we first propose to perform masked image modeling with denoising contrast, achieving the state-of-the-art performance on four downstream tasks [7, 24, 44] while getting rid of the off-the-shelf image tokenizers [29, 11]. This attempt unleashes the great potential of contrastive learning in self-supervised pre-training of vision Transformers [10]. We hope our work could revitalize contrastive learning and look forward to further research along this direction.

Limitations. The current version of ConMIM has the following limitations. (1) The intra-image inter-patch contrastive loss may carry some noise as there may exist semantically repetitive patches.

(2) We need twice forward operation in each iteration for encoding the full input and corrupted image. If we can reduce such operations to one time, we can save more computation for faster pre-training. (3) ConMIM achieves better performance on downstream detection and segmentation after intermediate fine-tuning. Although it is a common practice in NLP tasks [8], it would still limit the wide range of applications for ConMIM. In future work, we would like to try to address the above limitations, investigate other asymmetric designs for ConMIM, scale up the pre-trained models, and apply ConMIM on multimodal tasks to exploit its potential in universal representation learning.

Reproducibility. A fluctuation within $\pm 0.1\%$ accuracy may be observed on downstream classification when pre-training multiple times with different random seeds (we use 0 in default). We adopt 16 A100 GPUs for pre-training. ViT-Base requires around 3 days for 800 epochs and ViT-Small requires less than 1 day for 300 epochs. Pseudocode can be found in Appendix A. We will release our full code and pre-trained models upon acceptance.

References

- [1] Hangbo Bao, Li Dong, Songhao Piao, and Furu Wei. BEiT: BERT pre-training of image transformers. In *International Conference on Learning Representations*, 2022.
- [2] Mathilde Caron, Ishan Misra, Julien Mairal, Priya Goyal, Piotr Bojanowski, and Armand Joulin. Unsupervised learning of visual features by contrasting cluster assignments. *Advances in Neural Information Processing Systems*, 33:9912–9924, 2020.
- [3] Mathilde Caron, Hugo Touvron, Ishan Misra, Hervé Jégou, Julien Mairal, Piotr Bojanowski, and Armand Joulin. Emerging properties in self-supervised vision transformers. In *Proceedings of the IEEE/CVF International Conference on Computer Vision*, pages 9650–9660, 2021.
- [4] Ting Chen, Simon Kornblith, Mohammad Norouzi, and Geoffrey Hinton. A simple framework for contrastive learning of visual representations. In *International conference on machine learning*, pages 1597–1607. PMLR, 2020.
- [5] Xinlei Chen and Kaiming He. Exploring simple siamese representation learning. In *Proceedings of the IEEE/CVF Conference on Computer Vision and Pattern Recognition*, pages 15750–15758, 2021.
- [6] Xinlei Chen*, Saining Xie*, and Kaiming He. An empirical study of training self-supervised vision transformers. *arXiv preprint arXiv:2104.02057*, 2021.
- [7] Jia Deng, Wei Dong, Richard Socher, Li-Jia Li, Kai Li, and Li Fei-Fei. Imagenet: A large-scale hierarchical image database. In *2009 IEEE conference on computer vision and pattern recognition*, pages 248–255. Ieee, 2009.
- [8] Jacob Devlin, Ming-Wei Chang, Kenton Lee, and Kristina Toutanova. BERT: Pre-training of deep bidirectional transformers for language understanding. In *Proceedings of the 2019 Conference of the North American Chapter of the Association for Computational Linguistics: Human Language Technologies, Volume 1 (Long and Short Papers)*, pages 4171–4186, Minneapolis, Minnesota, June 2019. Association for Computational Linguistics.
- [9] Xiaoyi Dong, Jianmin Bao, Ting Zhang, Dongdong Chen, Weiming Zhang, Lu Yuan, Dong Chen, Fang Wen, and Nenghai Yu. Peco: Perceptual codebook for bert pre-training of vision transformers. *arXiv preprint arXiv:2111.12710*, 2021.
- [10] Alexey Dosovitskiy, Lucas Beyer, Alexander Kolesnikov, Dirk Weissenborn, Xiaohua Zhai, Thomas Unterthiner, Mostafa Dehghani, Matthias Minderer, Georg Heigold, Sylvain Gelly, Jakob Uszkoreit, and Neil Houlsby. An image is worth 16x16 words: Transformers for image recognition at scale. In *International Conference on Learning Representations*, 2021.
- [11] Patrick Esser, Robin Rombach, and Bjorn Ommer. Taming transformers for high-resolution image synthesis. In *Proceedings of the IEEE/CVF Conference on Computer Vision and Pattern Recognition*, pages 12873–12883, 2021.
- [12] Yuxin Fang, Li Dong, Hangbo Bao, Xinggang Wang, and Furu Wei. Corrupted image modeling for self-supervised visual pre-training. *arXiv preprint arXiv:2202.03382*, 2022.
- [13] Yuying Ge, Yixiao Ge, Xihui Liu, Dian Li, Ying Shan, Xiaohu Qie, and Ping Luo. Bridgeformer: Bridging video-text retrieval with multiple choice questions. *Proceedings of the IEEE/CVF conference on computer vision and pattern recognition*, 2022.
- [14] Golnaz Ghiasi, Yin Cui, Aravind Srinivas, Rui Qian, Tsung-Yi Lin, Ekin D Cubuk, Quoc V Le, and Barret Zoph. Simple copy-paste is a strong data augmentation method for instance segmentation. In *Proceedings of the IEEE/CVF Conference on Computer Vision and Pattern Recognition*, pages 2918–2928, 2021.

- [15] Jean-Bastien Grill, Florian Strub, Florent Altché, Corentin Tallec, Pierre Richemond, Elena Buchatskaya, Carl Doersch, Bernardo Avila Pires, Zhaohan Guo, Mohammad Gheshlaghi Azar, et al. Bootstrap your own latent—a new approach to self-supervised learning. *Advances in Neural Information Processing Systems*, 33:21271–21284, 2020.
- [16] Kaiming He, Xinlei Chen, Saining Xie, Yanghao Li, Piotr Dollár, and Ross Girshick. Masked autoencoders are scalable vision learners. *International Conference on Computer Vision and Pattern Recognition (CVPR)*, 2022.
- [17] Kaiming He, Haoqi Fan, Yuxin Wu, Saining Xie, and Ross Girshick. Momentum contrast for unsupervised visual representation learning. In *Proceedings of the IEEE/CVF conference on computer vision and pattern recognition*, pages 9729–9738, 2020.
- [18] Kaiming He, Georgia Gkioxari, Piotr Dollár, and Ross Girshick. Mask r-cnn. In *Proceedings of the IEEE international conference on computer vision*, pages 2961–2969, 2017.
- [19] Kaiming He, Xiangyu Zhang, Shaoqing Ren, and Jian Sun. Deep residual learning for image recognition. In *Proceedings of the IEEE conference on computer vision and pattern recognition*, pages 770–778, 2016.
- [20] Alex Krizhevsky, Ilya Sutskever, and Geoffrey E Hinton. Imagenet classification with deep convolutional neural networks. In F. Pereira, C.J. Burges, L. Bottou, and K.Q. Weinberger, editors, *Advances in Neural Information Processing Systems*, volume 25. Curran Associates, Inc., 2012.
- [21] Xiaotong Li, Yixiao Ge, Kun Yi, Zixuan Hu, Ying Shan, and Ling-Yu Duan. mc-beit: Multi-choice discretization for image bert pre-training. *arXiv preprint arXiv:2203.15371*, 2022.
- [22] Yanghao Li, Saining Xie, Xinlei Chen, Piotr Dollar, Kaiming He, and Ross Girshick. Benchmarking detection transfer learning with vision transformers. *arXiv preprint arXiv:2111.11429*, 2021.
- [23] Tsung-Yi Lin, Piotr Dollár, Ross Girshick, Kaiming He, Bharath Hariharan, and Serge Belongie. Feature pyramid networks for object detection. In *Proceedings of the IEEE conference on computer vision and pattern recognition*, pages 2117–2125, 2017.
- [24] Tsung-Yi Lin, Michael Maire, Serge Belongie, James Hays, Pietro Perona, Deva Ramanan, Piotr Dollár, and C Lawrence Zitnick. Microsoft coco: Common objects in context. In *European conference on computer vision*, pages 740–755. Springer, 2014.
- [25] Ze Liu, Yutong Lin, Yue Cao, Han Hu, Yixuan Wei, Zheng Zhang, Stephen Lin, and Baining Guo. Swin transformer: Hierarchical vision transformer using shifted windows. In *Proceedings of the IEEE/CVF International Conference on Computer Vision*, pages 10012–10022, 2021.
- [26] Ilya Loshchilov and Frank Hutter. Decoupled weight decay regularization. *arXiv preprint arXiv:1711.05101*, 2017.
- [27] Alec Radford, Karthik Narasimhan, Tim Salimans, and Ilya Sutskever. Improving language understanding by generative pre-training. 2018.
- [28] Alec Radford, Jeff Wu, Rewon Child, David Luan, Dario Amodei, and Ilya Sutskever. Language models are unsupervised multitask learners. 2019.
- [29] Aditya Ramesh, Mikhail Pavlov, Gabriel Goh, Scott Gray, Chelsea Voss, Alec Radford, Mark Chen, and Ilya Sutskever. Zero-shot text-to-image generation. In Marina Meila and Tong Zhang, editors, *Proceedings of the 38th International Conference on Machine Learning*, volume 139 of *Proceedings of Machine Learning Research*, pages 8821–8831. PMLR, 18–24 Jul 2021.
- [30] Byungseok Roh, Wuhyun Shin, Ildoo Kim, and Sungwoong Kim. Spatially consistent representation learning. In *Proceedings of the IEEE/CVF Conference on Computer Vision and Pattern Recognition*, pages 1144–1153, 2021.
- [31] Wenqi Shao, Yixiao Ge, Zhaoyang Zhang, Xuyuan Xu, Xiaogang Wang, Ying Shan, and Ping Luo. Dynamic token normalization improves vision transformer. *arXiv preprint arXiv:2112.02624*, 2021.
- [32] Mingxing Tan and Quoc Le. Efficientnet: Rethinking model scaling for convolutional neural networks. In *International conference on machine learning*, pages 6105–6114. PMLR, 2019.
- [33] Yonglong Tian, Chen Sun, Ben Poole, Dilip Krishnan, Cordelia Schmid, and Phillip Isola. What makes for good views for contrastive learning? *Advances in Neural Information Processing Systems*, 33:6827–6839, 2020.
- [34] Hugo Touvron, Matthieu Cord, Matthijs Douze, Francisco Massa, Alexandre Sablayrolles, and Hervé Jégou. Training data-efficient image transformers & distillation through attention. In *International Conference on Machine Learning*, pages 10347–10357. PMLR, 2021.
- [35] Aaron Van den Oord, Yazhe Li, and Oriol Vinyals. Representation learning with contrastive predictive coding. *arXiv e-prints*, pages arXiv–1807, 2018.

- [36] Alex Jinpeng Wang, Yixiao Ge, Guanyu Cai, Rui Yan, Xudong Lin, Ying Shan, Xiaohu Qie, and Mike Zheng Shou. Object-aware video-language pre-training for retrieval. *arXiv preprint arXiv:2112.00656*, 2021.
- [37] Xiao Wang, Haoqi Fan, Yuandong Tian, Daisuke Kihara, and Xinlei Chen. On the importance of asymmetry for siamese representation learning. *arXiv preprint arXiv:2204.00613*, 2022.
- [38] Xinlong Wang, Rufeng Zhang, Chunhua Shen, Tao Kong, and Lei Li. Dense contrastive learning for self-supervised visual pre-training. In *Proceedings of the IEEE/CVF Conference on Computer Vision and Pattern Recognition*, pages 3024–3033, 2021.
- [39] Chen Wei, Haoqi Fan, Saining Xie, Chao-Yuan Wu, Alan Yuille, and Christoph Feichtenhofer. Masked feature prediction for self-supervised visual pre-training. *arXiv preprint arXiv:2112.09133*, 2021.
- [40] Tete Xiao, Yingcheng Liu, Bolei Zhou, Yuning Jiang, and Jian Sun. Unified perceptual parsing for scene understanding. In *Proceedings of the European Conference on Computer Vision (ECCV)*, pages 418–434, 2018.
- [41] Tete Xiao, Colorado J Reed, Xiaolong Wang, Kurt Keutzer, and Trevor Darrell. Region similarity representation learning. In *Proceedings of the IEEE/CVF International Conference on Computer Vision*, pages 10539–10548, 2021.
- [42] Zhenda Xie, Yutong Lin, Zheng Zhang, Yue Cao, Stephen Lin, and Han Hu. Propagate yourself: Exploring pixel-level consistency for unsupervised visual representation learning. In *Proceedings of the IEEE/CVF Conference on Computer Vision and Pattern Recognition*, pages 16684–16693, 2021.
- [43] Zhenda Xie, Zheng Zhang, Yue Cao, Yutong Lin, Jianmin Bao, Zhuliang Yao, Qi Dai, and Han Hu. Simmim: A simple framework for masked image modeling. In *International Conference on Computer Vision and Pattern Recognition (CVPR)*, 2022.
- [44] Bolei Zhou, Hang Zhao, Xavier Puig, Sanja Fidler, Adela Barriuso, and Antonio Torralba. Scene parsing through ade20k dataset. In *Proceedings of the IEEE conference on computer vision and pattern recognition*, pages 633–641, 2017.
- [45] Jinghao Zhou, Chen Wei, Huiyu Wang, Wei Shen, Cihang Xie, Alan Yuille, and Tao Kong. Image BERT pre-training with online tokenizer. In *International Conference on Learning Representations*, 2022.

A Pseudo-code of ConMIM Pre-training

Algorithm 1 Pseudo-code of ConMIM pre-training in a PyTorch-like style.

```

# f: backbone encoder, e.g., vit-base model
# t: temperature, \tau in the paper
# m: momentum, \alpha in the paper

f_slow.params = f.params # initialize
for (x, mask) in loader: # load a mini-batch x with N samples
    # image preprocess with asymmetric perturbations
    x = aug_basic(x) # share same basic aug for paired inputs
    x_full = aug_strong(x)
    x_corrupted = x*(1-mask)+mask_token.expand_as(x)*mask # randomly mask 75% patches

    # build patch-level dynamic dictionaries with asymmetric models
    with torch.no_grad():
        keys = f_slow(x_full) # NxKxD, K is the number of patches
        feats = f(x_corrupted) # NxKxD

    # dictionary look-up with denoising contrastive loss (Eq.(3))
    sim = bmm(feats.view(N,K,D), keys.view(N,D,K)).view(-1,K) # (NxK)xK
    labels = range(K).repeat(N) # (NxK)
    mask = mask.view(-1) # (NxK)
    loss = CrossEntropyLoss(sim[mask]/t, labels[mask])

    # update model
    loss.backward()
    update(f.params)
    f_slow.params = (1-m)*f.params+m*f_slow.params

```

bmm: batch matrix multiplication

B Hyper-parameters

B.1 ConMIM Pre-training

Configuration	ViT-S/16 [10]	ViT-B/16 [10]
Layers	12	12
Hidden size	384	768
Attention heads	6	12
Attention head size		64
Patch size		16 × 16
Training epochs	300	800
Batch size		2048
Adam ϵ		1e-8
Adam β		(0.9, 0.98)
Peak learning rate		5e-4
Minimal learning rate		1e-5
Learning rate schedule		Cosine
Warmup epochs		10
Initial momentum coefficient α		0.996
Maximal momentum coefficient α		1
Momentum coefficient schedule		Cosine
Temperature τ		0.1
Stoch. depth	0.1	None
Gradient clipping		3
Dropout		None
Weight decay		0.05
Masking patch size	16	32
Basic Data Augment		RandomResizeAndCrop ColorJitter(0.4,0.4,0.2,0.1), GaussianBlur(0.1), Solarization(0.2)
Strong Data Augment		
Input resolution		224 × 224

Table 10: Hyper-parameters for ConMIM pre-training on ImageNet-1K [7].

B.2 Image Classification Fine-tuning

Configuration	ViT-S/16 [10]	ViT-B/16 [10]
Peak learning rate	{1e-3,2e-3,4e-3,5e-3}	
Batch size	1024	
Fine-tuning epochs	200	100
Warmup epochs	5	20
Layer-wise learning rate decay	0.8	0.65
Adam ϵ	1e-8	
Adam β	(0.9, 0.999)	
Minimal learning rate	1e-6	
Learning rate schedule	Cosine	
Repeated Aug	None	
Weight decay	0.05	
Label smoothing	0.1	
Stoch. depth	0.1	
Dropout	None	
Gradient clipping	None	
Erasing prob.	0.25	
Input resolution	224 \times 224 or 384 \times 384	
Rand Augment	9/0.5	
Mixup prob.	0.8	
Cutmix prob.	1.0	
Color jitter	0.4	

Table 11: Hyper-parameters for fine-tuning ConMIM on ImageNet-1K [7] classification.

B.3 Semantic Segmentation Fine-tuning

Configuration	ViT-S/16 [10]	ViT-B/16 [10]
Peaking learning rate	{1e-5,3e-5,5e-5,7e-5}	
Fine-tuning steps	160K	
Batch size	16	
Adam ϵ	1e-8	
Adam β	(0.9, 0.999)	
Layer-wise learning rate decay	0.9	
Minimal learning rate	0	
Learning rate schedule	Linear	
Warmup steps	1500	
Dropout	None	
Stoch. depth	0.1	
Weight decay	0.05	
Input resolution	512 \times 512	
Position embedding	Relative	
Position embedding interpolate	Bilinear	

Table 12: Hyper-parameters for fine-tuning ConMIM on ADE20K [44] semantic segmentation.

B.4 Object Detection and Instance Segmentation Fine-tuning

Configuration	ViT-S/16 [10]	ViT-B/16 [10]
Fine-tuning epochs		25
Peaking learning rate		1e-4
Learning rate decay		cosine
Adam ϵ		1e-8
Adam β		(0.9, 0.999)
Dropout		None
Stoch. depth		0.1
Weight decay		0.1
Batch size		64
Input size		1024 × 1024
Position embedding		Abs. + Rel.
Augmentation		LSJ(0.1, 2.0)

Table 13: Hyper-parameters for fine-tuning ConMIM on COCO [24] object detection and instance segmentation.

C Visualization

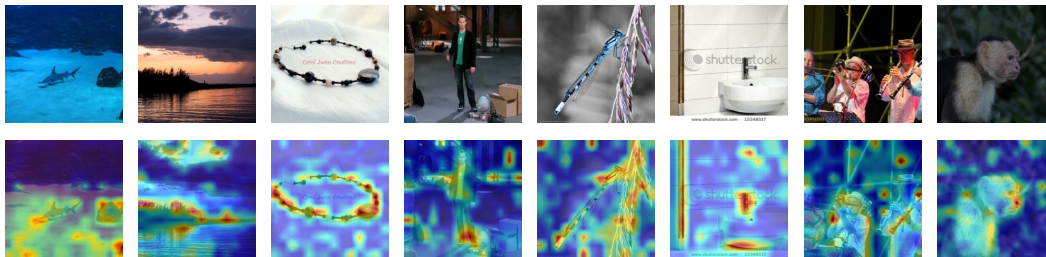


Figure 3: Visualize the self-attention map between [CLS] token and local tokens of the ViT-B/16 [10] model pre-trained with ConMIM on ImageNet-1K [7]. Self-attention maps out of 12 attention heads are averaged. It can be observed that ConMIM-pretrained models are locally discriminative and aware of the visual context.